Acta Cryst E CRYSTALLOGRAPHIC COMMUNICATIONS

ISSN 2056-9890

Synthesis and crystal structure of a 6-chloronicotinate salt of a one-dimensional cationic nickel(II) coordination polymer with 4,4′-bipyridine

Nives Politeo,[a] Mateja Pisačić,[b] Marijana Đaković,[b] Vesna Sokol[a]* and Boris-Marko Kukovec[a]

[a]Department of Physical Chemistry, Faculty of Chemistry and Technology, University of Split, Ruđera Boškovića 35, HR-21000 Split, Croatia, and [b]Department of Chemistry, Faculty of Science, University of Zagreb, Horvatovac, 102a, HR-10000 Zagreb, Croatia. *Correspondence e-mail: vsokol@ktf-split.hr

Received 18 March 2020
Accepted 26 March 2020

Edited by W. T. A. Harrison, University of Aberdeen, Scotland

Keywords: nickel(II); 6-chloronicotinic acid; 4,4′-bipyridine; coordination polymer; hydrogen-bond motif; crystal structure.

CCDC reference: 1992951

Supporting information: this article has supporting information at journals.iucr.org/e

A 6-chloronicotinate (6-Clnic) salt of a one-dimensional cationic nickel(II) coordination polymer with 4,4′-bipyridine (4,4′-bpy), namely, *catena*-poly-[[[tetraaquanickel(II)]-μ-4,4′-bipyridine-κ^2N:N'] bis(6-chloronicotinate) tetrahydrate], $\{[Ni(C_{10}H_8N_2)(H_2O)_4](C_6H_3ClNO_2)_2{\cdot}4H_2O\}_n$ or $\{[Ni(4,4'\text{-bpy})(H_2O)_4](6\text{-Clnic})_2{\cdot}4H_2O\}_n$, (**1**), was prepared by the reaction of nickel(II) sulfate heptahydrate, 6-chloronicotinic acid and 4,4′-bipyridine in a mixture of water and ethanol. The molecular structure of **1** comprises a one-dimensional polymeric $\{[Ni(4,4'\text{-bpy})(H_2O)_4]^{2+}\}_n$ cation, two 6-chloronicotinate anions and four water molecules of crystallization per repeating polymeric unit. The nickel(II) ion in the polymeric cation is octahedrally coordinated by four water molecule O atoms and by two 4,4′-bipyridine N atoms in the *trans* position. The 4,4′-bipyridine ligands act as bridges and, thus, connect the symmetry-related nickel(II) ions into an infinite one-dimensional polymeric chain extending along the *b*-axis direction. In the extended structure of **1**, the polymeric chains of $\{[Ni(4,4'\text{-bpy})(H_2O)_4]^{2+}\}_n$, the 6-chloronicotinate anions and the water molecules of crystallization are assembled into an infinite three-dimensional hydrogen-bonded network *via* strong O—H···O and O—H···N hydrogen bonds, leading to the formation of the representative hydrogen-bonded ring motifs: tetrameric $R_4^2(8)$ and $R_4^4(10)$ loops, a dimeric $R_2^2(8)$ loop and a pentameric $R_5^4(16)$ loop.

1. Chemical context

Functional coordination polymers have attracted great interest in recent years, mostly due to their aesthetics and many interesting properties such as catalytic, magnetic and luminescent, potential for use in gas storage and separation, molecular sensing (Mueller *et al.*, 2006; Bosch *et al.*, 2017; Zhang *et al.*, 2015; Zeng *et al.*, 2014, 2016; Douvali *et al.*, 2015; Xu *et al.*, 2017; Zhou *et al.*, 2017).

The organic ligands, used as building blocks in the construction of coordination polymers, need to be multifunctional, which is evident from the position, coordination ability and steric hindrance of their donor atoms and/or groups. The design of functional coordination polymers with the desired structures is not always straightforward and is strongly dependent on the experimental conditions including the type of solvents, starting metal salts, additional ligands, temperature, hydrothermal conditions and pH value (Li *et al.*, 2016; Zhou *et al.*, 2016; Gu *et al.*, 2016). Aromatic carboxylic acids with additional functional groups have become popular in the design of coordination polymers. The main reasons are

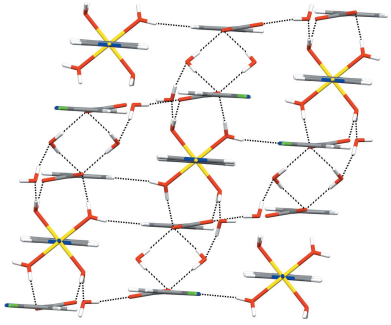

the many possible and unpredictable coordination modes of this type of ligand and their affinity for participation in supramolecular interactions (Gu *et al.*, 2016, 2017, 2018; Wang *et al.*, 2016; Zhang *et al.*, 2019).

The metal complexes of chlorinated analogues of the nicotinate anion (*e.g.* 2-chloronicotinate and 5-chloronicotinate) have not been particularly well-studied [as of March 2020, there are around 20 crystal structures in the CSD (Groom *et al.*, 2016) for each ligand]. Furthermore, no metal complexes of the 4-chloronicotinate anion have been reported. The crystal structures of only three metal complexes of 6-chloronicotinate (6-Clnic) are known so far (Xia *et al.*, 2012*a*,*b*; Li *et al.*, 2006). Recently, we have reported the synthesis, crystal structure and properties of a one-dimensional nickel(II) coordination polymer with mixed ligands: 6-fluoronicotinate as the main ligand and 4,4′-bipyridine (4,4′-bpy) as the supporting ligand (Politeo *et al.*, 2020).

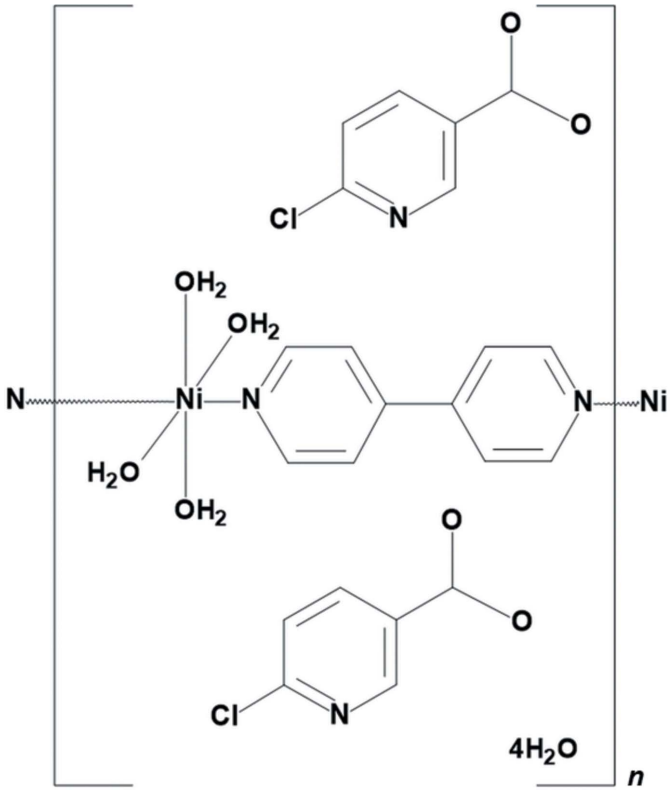

In a continuation of our work on coordination polymers with mixed ligands, we set out to prepare a similar coordination polymer with 6-chlorinicotinate and 4,4′-bipyridine, as we did with 6-fluoronicotinate (Politeo *et al.*, 2020). Therefore, we carried out the synthesis and crystallization under the same experimental conditions (in a mixture of water and ethanol and with the same molar ratios of the nickel(II) sulfate and ligands), in hope that the analogous nickel(II) coordination polymer could be obtained. We also wanted to examine the influence of the possible weak intermolecular interactions involving the chlorine atoms (*e.g.* C—H···Cl interactions) on the assembly of the polymeric chains in the crystal packing,

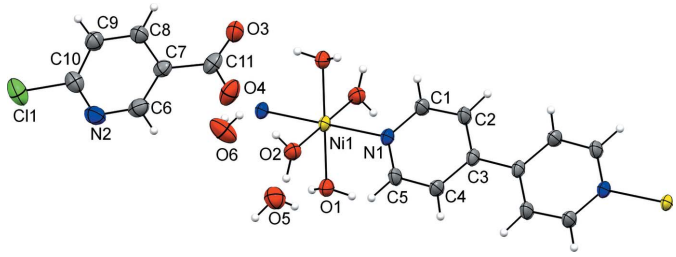

Figure 1
The molecular structure of **1**, comprising a $\{[Ni(4,4'\text{-bpy})(H_2O)_4]^{2+}\}_n$ cation, 6-chloronicotinate anion and water molecules of crystallization. The atomic numbering scheme of the asymmetric unit is shown and displacement ellipsoids are drawn at the 40% probability level.

especially since the analogous C—H···F interactions were not found in the crystal packing of the nickel(II) coordination polymer with 6-fluoronicotinate (Politeo *et al.*, 2020). Unfortunately, we were not able to prepare the desired nickel(II) coordination polymer under these experimental conditions, but instead we obtained a 6-chloronicotinate salt of a one-dimensional cationic nickel(II) coordination polymer with 4,4′-bipyridine, namely the title compound, $\{[Ni(4,4'\text{-bpy})(H_2O)_4](6\text{-Clnic})_2{\cdot}4H_2O\}_n$, (**1**).

2. Structural commentary

As the nickel(II) ion is situated on an inversion center, the asymmetric unit of **1** contains one half of a nickel(II) ion, two coordinated water molecules, one 6-chloronicotinate ligand, one half of a 4,4′-bipyridine ligand and two water molecules of crystallization (Fig. 1). Therefore, the molecular structure of **1** comprises a one-dimensional polymeric $\{[Ni(4,4'\text{-bpy})(H_2O)_4]^{2+}\}_n$ cation and two 6-chloronicotinate anions and four uncoordinated water molecules per repeating polymeric unit. The nickel(II) ion in the polymeric $\{[Ni(4,4'\text{-bpy})(H_2O)_4]^{2+}\}_n$ cation is octahedrally coordinated by four water molecule O atoms (O1, O2, O1^{i} and O2^{i}) [symmetry code: (i) $-x+1, -y+1, -z+1$] and by two 4,4′-bipyridine N atoms (N1 and N1^{i}) in the *trans* position (N1^{i}—Ni1—N1 = 180°). The 4,4′-bipyridine ligands act as bridges and, thus, connect the symmetry-related nickel(II) ions into infinite one-dimensional polymeric chains extending along the *b*-axis direction (Fig. 2).

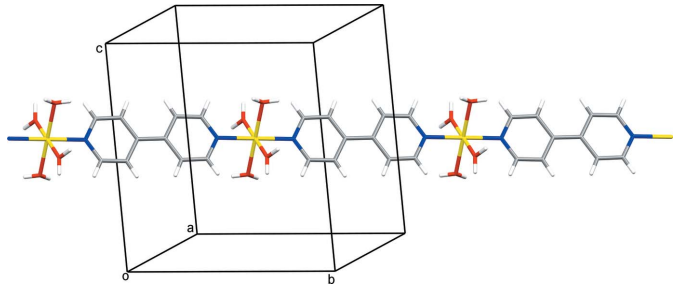

Figure 2
The infinite one-dimensional polymeric chain of $\{[Ni(4,4'\text{-bpy})(H_2O)_4]^{2+}\}_n$ cations in **1**, extending along the *b*-axis direction.

The octahedral coordination environment around the nickel(II) ion is only slightly distorted, as indicated by the angles for the *cis* pairs of the ligating atoms [89.00 (5)–91.00 (5)°]. The Ni1—O1 and Ni1—O2 bond lengths [2.0643 (15) Å and 2.0850 (13) Å, respectively] are very similar to each other and comparable to those seen in the related structures containing $\{[Ni(4,4'\text{-bpy})(H_2O)_4]^{2+}\}_n$ cation. The Ni—N1 bond length [2.0715 (14) Å] is also in agreement with those reported for the structures containing the $\{[Ni(4,4'\text{-bpy})(H_2O)_4]^{2+}\}_n$ cation (Zheng *et al.*, 2002; Gong *et al.*, 2009; Li, 2011; Gao *et al.*, 2016; Sun *et al.*, 2013; Wang *et al.*, 2006; Sanram *et al.*, 2016; Hu & Zhang, 2010).

The 4,4′-bypyridine ring is not coplanar with either coordinated water molecule O1 or O2 atoms and is rotated about the Ni1—N1 bond (by approximately 2°), as is evident from the torsion angles Ni1—N1—C5—C4 and Ni1—N1—C1—C2 [177.75 (16) and −177.83 (16)°, respectively].

3. Supramolecular features

The extended structure of **1** features strong O—H···O and O—H···N hydrogen bonds, weak C—H···O hydrogen bonds (Table 1) and π–π interactions [*Cg*2···*Cg*2; where *Cg*2 is the centroid of the 6-chloronicotinate pyridine ring N2/C6–C10; *Cg*2···*Cg*2 distance = 3.6769 (12) Å; dihedral angle between the planes = 0.00 (10)°; slippage = 1.085 Å]. The strong hydrogen bonds link the polymeric chains of $\{[Ni(4,4'\text{-bpy})(H_2O)_4]^{2+}\}_n$, the 6-chloronicotinate anions and the water molecules of crystallization into an infinite three-dimensional network. The structure can be better analyzed if viewed down the *b*-axis direction (the direction along which the polymeric chain of $\{[Ni(4,4'\text{-bpy})(H_2O)_4]^{2+}\}_n$ runs). In that projection, the polymeric chains can be regarded as monomeric molecules that are interconnected with the 6-chloronicotinate anions and water molecules of crystallization into a hydrogen-bonded framework (Fig. 3). The polymeric chains are exclusively hydrogen-bonded to 6-chloronicotinate anions and water molecules, whilst the 6-chloronicotinate anions are additionally assembled by π–π interactions between symmetry-related 6-chloronicotinate pyridine rings.

Table 1
Hydrogen-bond geometry (Å, °).

D—H···*A*	*D*—H	H···*A*	*D*···*A*	*D*—H···*A*
O1—H11···O3^{i}	0.81 (1)	1.95 (1)	2.756 (2)	175 (2)
O1—H12···O5	0.82 (1)	1.90 (1)	2.715 (2)	175 (2)
O2—H21···N2^{ii}	0.81 (1)	2.08 (1)	2.885 (2)	172 (2)
O2—H22···O4	0.81 (1)	1.96 (1)	2.757 (2)	169 (2)
O5—H51···O3^{iii}	0.82 (1)	1.96 (1)	2.776 (2)	172 (3)
O5—H52···O6^{iv}	0.82 (1)	2.01 (1)	2.790 (3)	160 (3)
O6—H61···O4	0.82 (1)	1.94 (1)	2.753 (2)	177 (3)
O6—H62···O4^{v}	0.81 (1)	2.23 (1)	3.035 (3)	174 (3)
C4—H4···O6^{ii}	0.93	2.40	3.288 (3)	160
C9—H9···O5^{vi}	0.93	2.53	3.447 (3)	169

Symmetry codes: (i) $-x+1, -y+1, -z+1$; (ii) $-x+\frac{1}{2}, y+\frac{1}{2}, -z+\frac{3}{2}$; (iii) $x+\frac{1}{2}, -y+\frac{1}{2}, z+\frac{1}{2}$; (iv) $x+1, y, z$; (v) $-x, -y+1, -z+1$; (vi) $-x+1, -y, -z+1$.

There are some representative supramolecular ring motifs within the hydrogen-bonded framework of **1**: tetrameric $R_4^2(8)$ and $R_4^4(10)$ motifs, a dimeric $R_2^2(8)$ motif and a pentameric $R_5^4(16)$ motif (Fig. 4). The tetrameric $R_4^2(8)$ motif is formed

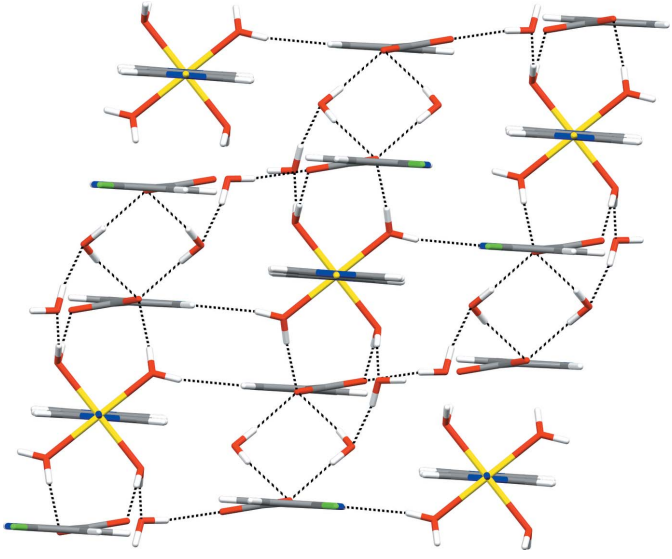

Figure 3
A fragment of the infinite hydrogen-bonded network of **1** viewed along the *b*-axis direction. The polymeric chains of $\{[Ni(4,4'\text{-bpy})(H_2O)_4]^{2+}\}_n$ (represented as monomeric molecules in this projection), 6-chloronicotinate anions and water molecules of crystallization are connected by O—H···O and O—H···N hydrogen bonds (represented by dotted lines) within the hydrogen-bonded framework.

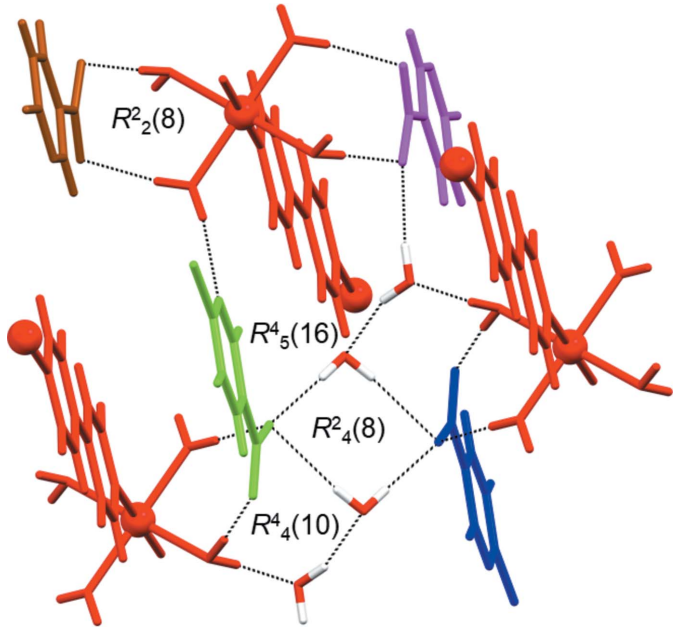

Figure 4
The representative hydrogen-bonded ring motifs (shown by dotted lines) found within the hydrogen-bonded framework of **1**, *viz*. the tetrameric $R_4^2(8)$ and $R_4^4(10)$ motifs, a dimeric $R_2^2(8)$ motif and a pentameric $R_5^4(16)$ motif. The polymeric chains of $\{[Ni(4,4'\text{-bpy})(H_2O)_4]^{2+}\}_n$ are represented as momomeric molecules and shown in red, and various symmetry-related 6-chloronicotinate anions are shown in brown, green, blue and pink (see text).

between two water molecules of crystallization and two 6-chloronicotinate anions (indicated in blue and green); each 6-chloronicotinate anion is linked *via* a single carboxylate O atom. The tetrameric $R_4^4(10)$ motif is formed between the $[Ni(4,4'\text{-bpy})(H_2O)_4]^{2+}\}_n$ cation, a 6-chloronicotinate anion (indicated in red and green, respectively) and two water molecules of crystallization; the cation participates in this motif *via* a coordinated water O atom and the 6-chloronicotinate anion *via* both carboxylate O atoms. The dimeric $R_2^2(8)$ motif is formed between the $\{[Ni(4,4'\text{-bpy})(H_2O)_4]^{2+}\}_n$ cation and the 6-chloronicotinate anion (indicated in red and brown, respectively); the cation is involved in this motif *via* two coordinated water O atoms and the 6-chloronicotinate anion *via* both carboxylate O atoms. Finally, the pentameric $R_5^4(16)$ motif is composed of the $\{[Ni(4,4'\text{-bpy})(H_2O)_4]^{2+}\}_n$ cation, two 6-chloronicotinate anions (indicated in red, green and pink) and two water molecules of crystallization; the cation participates in this motif *via* two coordinated water O atoms, one 6-chloronicotinate anion (shown in green) *via* both carboxylate O atoms and the pyridine N atom and the other 6-chloronicotinate anion (shown in pink) *via* its carboxylate O atom only (Fig. 4). Both coordinated water molecules and water molecules of crystallization participate in the formation of motifs as single- and double-proton donors [coordinated water molecules as single-proton donors in the $R_5^4(16)$ and $R_2^2(8)$ motifs and double-proton donors in the $R_4^4(10)$ motif only; water molecules of crystallization as single-proton donors in the $R_5^4(16)$ motifs and $R_4^4(10)$ motifs and double-proton donors in the $R_5^4(16)$ and $R_4^2(8)$ motifs]. The water molecules of crystallization also participate in some of these motifs [$R_5^4(16)$ and $R_4^4(10)$] as single-proton acceptors. The 6-chloronicotinate pyridine N atoms act as single-proton acceptors in the $R_5^4(16)$ motif only, whilst the carboxylate O atoms act as both single- and double-proton acceptors [single in the $R_5^4(16)$, $R_2^2(8)$ and $R_4^4(10)$ motifs and double in the $R_5^4(16)$ and $R_4^2(8)$ motifs]. Two weak C—H···O interactions are also observed (Table 1).

There are no weak C—H···Cl interactions in the extended structure of **1**; we hoped that these interactions could have an impact on the assembly of the polymeric chains within the hydrogen-bonding framework of **1**: the polymeric chains do not contain the 6-chloronicotinate ligands, but the uncoordinated 6-chloronicotinate anions could still participate in these interactions. However, the possible C—H···Cl interactions are most probably hindered by the extensive hydrogen bonding, involving strong O—H···O and O—H···N hydrogen bonds, which is reflected in the formation of various hydrogen-bonded motifs. This was expected because of the participation of the water molecules of crystallization in the crystal packing of **1**, since the compound was crystallized from a mixed water–ethanol solution.

4. Database survey

Our aim in this work was to prepare a nickel(II) coordination polymer with the mixed ligands 6-chloronicotinate and 4,4′-bipyridine. However, we obtained a cationic nickel(II) coordination polymer with 4,4′-bipyridine, $\{[Ni(4,4'\text{-bpy})(H_2O)_4]^{2+}\}_n$. The 6-chloronicotinate is not coordinated to the metal ion, but acts as a counter-ion. This was surprising, as we expected to obtain a coordination polymer similar to the one obtained with the closely related 6-fluoronicotinate anion under the same experimental conditions (Politeo *et al.*, 2020). The polymeric $\{[Ni(4,4'\text{-bpy})(H_2O)_4]^{2+}\}_n$ cation is already well known from the literature, as it crystallizes with various carboxylate anions such as fumarate (Zheng *et al.*, 2002), 3-[4-(carboxymethoxy) phenyl]propanoate (Gong *et al.*, 2009), 3,3′-(*p*-phenylene)diacrylate (Li, 2011), 2-carboxy-4-[4-(3-carboxy-4-carboxylatophenoxy)phenoxy]benzoate (Gao *et al.*, 2016), 3-(4-carboxyphenyl)propanoate (Sun *et al.*, 2013), 1,2,4,5-benzenetetracarboxylate (Wang *et al.*, 2006), 1,4-phenylenedipropanoate (Sanram *et al.*, 2016) and 2,3-naphthalenedicarboxylate (Hu & Zhang, 2010).

5. PXRD and thermal analysis

The experimental and calculated PXRD traces of **1** (Fig. 5) match nicely, indicating the phase purity of the bulk of **1**.

Compound **1** is thermally stable only up to 40°C (Fig. S1 in the supporting information). Both the coordinated (four) and uncoordinated (four) water molecules were released in the same step (observed mass loss 20.3%, calculated 21.4%), with a pronounced endothermic peak in the DSC curve at 90°C. The thermal decomposition of **1** continues in a broad step (observed mass loss 55.2%) in the wide temperature range of 145–590°C (with two small peaks in the DSC curve at 216 and 480°C), which probably corresponds to the complete degradation of **1**. The remaining residue at 600°C is most probably NiO.

6. Materials and methods

All chemicals for the synthesis were purchased from commercial sources (Merck) and used as received without further purification. The IR spectrum was obtained in the

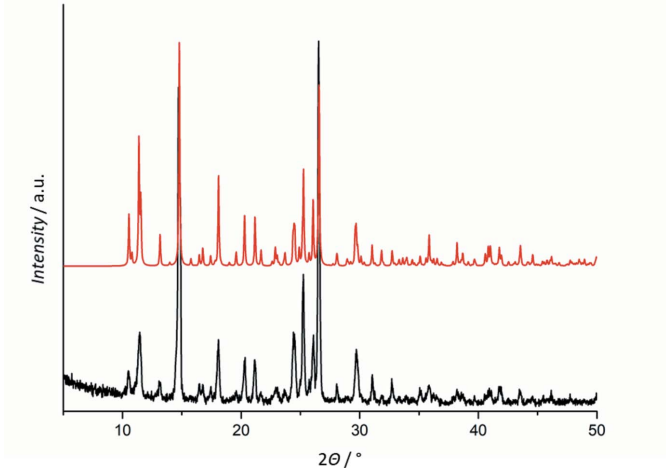

Figure 5
Experimental (bottom) and calculated (top) PXRD traces for **1**.

Table 2
Experimental details.

Crystal data	
Chemical formula	$\{[Ni(C_{10}H_8N_2)(H_2O)_4]\cdot(C_6H_3ClNO_2)_2\cdot 4H_2O\}_n$
M_r	672.11
Crystal system, space group	Monoclinic, $P2_1/n$
Temperature (K)	296
a, b, c (Å)	10.7997 (3), 11.2319 (2), 12.0225 (3)
β (°)	95.184 (2)
V (Å^3)	1452.38 (6)
Z	2
Radiation type	Mo $K\alpha$
μ (mm^{-1})	0.92
Crystal size (mm)	0.24 × 0.18 × 0.16
Data collection	
Diffractometer	Oxford Diffraction Xcalibur2 diffractometer with Sapphire 3 CCD detector
Absorption correction	Multi-scan (*CrysAlis PRO*; Rigaku OD, 2018)
T_{min}, T_{max}	0.927, 1.000
No. of measured, independent and observed [$I > 2\sigma(I)$] reflections	11778, 2541, 2144
R_{int}	0.025
$(\sin\theta/\lambda)_{max}$ (Å^{-1})	0.595
Refinement	
$R[F^2 > 2\sigma(F^2)]$, $wR(F^2)$, S	0.029, 0.074, 1.07
No. of reflections	2541
No. of parameters	211
No. of restraints	12
H-atom treatment	H atoms treated by a mixture of independent and constrained refinement
$\Delta\rho_{max}$, $\Delta\rho_{min}$ (e Å^{-3})	0.23, −0.23

Computer programs: *CrysAlis PRO* (Rigaku OD, 2018), *SHELXT* (Sheldrick, 2015*a*), *SHELXL2018/3* (Sheldrick, 2015*b*) and *Mercury* (Macrae *et al.*, 2020).

range 4000–400 cm^{-1} on a Perkin–Elmer Spectrum Two™ FTIR spectrometer in the ATR mode. The PXRD trace was recorded on a Philips PW 1850 diffractometer, Cu $K\alpha$ radiation, voltage 40 kV, current 40 mA, in the angle range 5–50° (2θ) with a step size of 0.02°. Simultaneous TGA/DSC measurements were performed at a heating rate of 10°C min^{-1} in the temperature range 25–600°C, under a nitrogen flow of 50 ml min^{-1} on a Mettler–Toledo TGA/DSC 3+ instrument. Approximately 2 mg of sample was placed in a standard alumina crucible (70 µl).

7. Synthesis and crystallization

6-Chloronicotinic acid (0.0525 g, 0.3332 mmol) was dissolved in distilled water (5 ml) using an ultrasonic water bath, 4,4′-bipyridine (0.0244 g, 0.1562 mmol) was dissolved in ethanol (2 ml) and nickel(II) sulfate heptahydrate (0.0446 g, 0.1588 mmol) was dissolved in distilled water (2 ml). The solutions of the two ligands were first mixed together under stirring. The resulting solution was then slowly added to the nickel(II) sulfate solution under stirring. The pH of the final solution was adjusted to 7 by adding an ammonia solution dropwise. The obtained, clear solution was left to slowly evaporate at room temperature for approximately three weeks until light-green crystals of **1**, suitable for X-ray diffraction measurements, were obtained, which were collected by filtration, washed with their mother liquor and dried *in vacuo*. Yield: 0.0496 g (46%). Selected IR bands (ATR) (ν, cm^{-1}): 3376 [ν(O—H)], 3078, 3059 [ν(C—H)], 1615 [ν(C=O)], 1579, 1539, 1419, 1388, 1360 [ν(C—C), ν(C—N)] (Fig. S2, Table S1 in the supporting information).

8. Refinement

Crystal data, data collection and structure refinement details are summarized in Table 2. C-bound H atoms were positioned geometrically and refined using riding model [C—H = 0.93 Å, U_{iso}(H) = 1.2U_{eq}(C) for the aromatic H atoms]. The H atoms belonging to the water molecules were found in the difference-Fourier maps. The O—H distance was restrained to an average value of 0.82 Å using DFIX and DANG instructions. The isotropic U_{iso}(H) values were also fixed [U_{iso}(H) = 1.2U_{eq}(O)].

The highest difference peak is 0.86 Å away from the O4 atom and the deepest difference hole is 0.84 Å away from the Cl1 atom.

Funding information

This research was supported by a Grant from the Foundation of the Croatian Academy of Sciences and Arts for 2019 and by University of Split institutional funding.

References

Bosch, M., Yuan, S., Rutledge, W. & Zhou, H.-C. (2017). *Acc. Chem. Res.* **50**, 857–865.
Douvali, A., Tsipis, A. C., Eliseeva, S. V., Petoud, S., Papaefstathiou, G. S., Malliakas, C. D., Papadas, I., Armatas, G. S., Margiolaki, I., Kanatzidis, M. G., Lazarides, T. & Manos, M. J. (2015). *Angew. Chem. Int. Ed.* **54**, 1651–1656.
Gao, P., Bai, H., Bing, Y.-Y. & Hu, M. (2016). *Solid State Sci.* **52**, 118–125.
Gong, Y.-N., Liu, C.-B., Huang, D.-H. & Xiong, Z.-Q. (2009). *Z. Kristallogr. New Cryst. Struct.* **224**, 421–422.
Groom, C. R., Bruno, I. J., Lightfoot, M. P. & Ward, S. C. (2016). *Acta Cryst.* B**72**, 171–179.
Gu, J., Cui, Y., Liang, X., Wu, J., Lv, D. & Kirillov, A. M. (2016). *Cryst. Growth Des.* **16**, 4658–4670.
Gu, J.-Z., Cai, Y., Liang, X.-X., Wu, J., Shi, Z.-F. & Kirillov, A. M. (2018). *CrystEngComm*, **20**, 906–916.
Gu, J.-Z., Liang, X.-X., Cai, Y., Wu, J., Shi, Z.-F. & Kirillov, A. M. (2017). *Dalton Trans.* **46**, 10908–10925.
Hu, M. & Zhang, Q. (2010). *Z. Kristallogr. New Cryst. Struct.* **225**, 155–156.
Li, F.-H., Yin, H.-D., Sun, L., Zhao, Q. & Liu, W.-L. (2006). *Acta Cryst.* E**62**, m1117–m1118.
Li, J.-J., Fan, T.-T., Qu, X.-L., Han, H.-L. & Li, X. (2016). *Dalton Trans.* **45**, 2924–2935.
Li, N.-Y. (2011). *Acta Cryst.* E**67**, m1397.
Macrae, C. F., Sovago, I., Cottrell, S. J., Galek, P. T. A., McCabe, P., Pidcock, E., Platings, M., Shields, G. P., Stevens, J. S., Towler, M. & Wood, P. A. (2020). *J. Appl. Cryst.* **53**, 226–235.
Mueller, U., Schubert, M., Teich, F., Puetter, H., Schierle-Arndt, K. & Pastré, J. (2006). *J. Mater. Chem.* **16**, 626–636.

Politeo, N., Pisačić, M., Đaković, M., Sokol, V. & Kukovec, B.-M. (2020). *Acta Cryst.* E**76**, 500–505.
Rigaku OD (2018). *CrysAlis PRO*. Rigaku Oxford Diffraction, Yarnton, England.
Sanram, S., Boonmak, J. & Youngme, S. (2016). *Polyhedron*, **119**, 151–159.
Sheldrick, G. M. (2015*a*). *Acta Cryst.* A**71**, 3–8.
Sheldrick, G. M. (2015*b*). *Acta Cryst.* C**71**, 3–8.
Sun, C.-Y., Li, W.-J. & Che, P. (2013). *Z. Anorg. Allg. Chem.* **639**, 129–133.
Wang, H.-H., Yang, H.-Y., Shu, C.-H., Chen, Z.-Y., Hou, L. & Wang, Y.-Y. (2016). *Cryst. Growth Des.* **16**, 5394–5402.
Wang, X.-L., Qin, C. & Wang, E.-B. (2006). *Cryst. Growth Des.* **6**, 439–443.
Xia, Q.-H., Guo, Z.-F., Liu, L., Lv, J.-Q. & Li, B. (2012*a*). *Acta Cryst.* E**68**, m1393.
Xia, Q.-H., Zhang, Y., Liu, L., Shi, L.-F. & Li, B. (2012*b*). *Acta Cryst.* E**68**, m1394.
Xu, M., Yuan, S., Chen, X.-Y., Chang, Y.-J., Day, G., Gu, Z.-Y. & Zhou, H.-C. (2017). *J. Am. Chem. Soc.* **139**, 8312–8319.
Zeng, M.-H., Yin, Z., Liu, Z.-H., Xu, H.-B., Feng, Y.-C., Hu, Y.-Q., Chang, L.-X., Zhang, Y.-X., Huang, J. & Kurmoo, M. (2016). *Angew. Chem. Int. Ed.* **55**, 11407–11411.
Zeng, M.-H., Yin, Z., Tan, Y.-X., Zhang, W.-X., He, Y.-P. & Kurmoo, M. (2014). *J. Am. Chem. Soc.* **136**, 4680–4688.
Zhang, W.-X., Liao, P.-Q., Lin, R.-B., Wei, Y.-S., Zeng, M.-H. & Chen, X.-M. (2015). *Coord. Chem. Rev.* **293–294**, 263–278.
Zhang, Y.-X., Lin, H., Wen, Y. & Zhu, Q.-L. (2019). *Cryst. Growth Des.* **19**, 1057–1063.
Zheng, Y.-Q., Kong, Z.-P. & Lin, J.-L. (2002). *Z. Kristallogr. New Cryst. Struct.* **217**, 195–196.
Zhou, H.-F., He, T., Yue, K.-F., Liu, Y.-L., Zhou, C.-S., Yan, N. & Wang, Y.-Y. (2016). *Cryst. Growth Des.* **16**, 3961–3968.
Zhou, Z., He, C., Yang, L., Wang, Y., Liu, T. & Duan, C. (2017). *ACS Catal.* **7**, 2248–2256.

supporting information

Acta Cryst. (2020). E**76**, 599-604 [https://doi.org/10.1107/S2056989020004193]

Synthesis and crystal structure of a 6-chloronicotinate salt of a one-dimensional cationic nickel(II) coordination polymer with 4,4′-bipyridine

Nives Politeo, Mateja Pisačić, Marijana Đaković, Vesna Sokol and Boris-Marko Kukovec

Computing details

Data collection: *CrysAlis PRO* (Rigaku OD, 2018); cell refinement: *CrysAlis PRO* (Rigaku OD, 2018); data reduction: *CrysAlis PRO* (Rigaku OD, 2018); program(s) used to solve structure: SHELXT (Sheldrick, 2015*a*); program(s) used to refine structure: *SHELXL2018/3* (Sheldrick, 2015*b*); molecular graphics: *Mercury* (Macrae *et al.*, 2020); software used to prepare material for publication: *SHELXL2018/3* (Sheldrick, 2015*b*).

catena-Poly[[[tetraaquanickel(II)]-μ-4,4′-bipyridine-κ²N:N′] bis(6-chloronicotinate) tetrahydrate]

Crystal data

$[Ni(C_{10}H_8N_2)(H_2O)_4](C_6H_3ClNO_2)_2{\cdot}4H_2O$
M_r = 672.11
Monoclinic, $P2_1/n$
a = 10.7997 (3) Å
b = 11.2319 (2) Å
c = 12.0225 (3) Å
β = 95.184 (2)°
V = 1452.38 (6) Å^3
Z = 2
$F(000)$ = 696
D_x = 1.537 Mg m^{-3}
Mo $K\alpha$ radiation, λ = 0.71073 Å
Cell parameters from 6296 reflections
θ = 4.4–32.2°
μ = 0.92 mm^{-1}
T = 296 K
Prism, light-green
0.24 × 0.18 × 0.16 mm

Data collection

Oxford Diffraction Xcalibur2 diffractometer with Sapphire 3 CCD detector
ω–scan
Absorption correction: multi-scan (CrysAlisPro; Rigaku OD, 2018)
T_{min} = 0.927, T_{max} = 1.000
11778 measured reflections
2541 independent reflections
2144 reflections with $I > 2\sigma(I)$
R_{int} = 0.025
θ_{max} = 25.0°, θ_{min} = 4.2°
h = −12→12
k = −13→13
l = −14→14

Refinement

Refinement on F^2
Least-squares matrix: full
$R[F^2 > 2\sigma(F^2)]$ = 0.029
$wR(F^2)$ = 0.074
S = 1.07
2541 reflections
211 parameters
12 restraints
Primary atom site location: dual
Hydrogen site location: mixed
H atoms treated by a mixture of independent and constrained refinement
$w = 1/[\sigma^2(F_o^2) + (0.0367P)^2 + 0.3591P]$ where $P = (F_o^2 + 2F_c^2)/3$
$(\Delta/\sigma)_{max} < 0.001$
$\Delta\rho_{max}$ = 0.23 e Å^{-3}
$\Delta\rho_{min}$ = −0.23 e Å^{-3}

Special details

Geometry. All esds (except the esd in the dihedral angle between two l.s. planes) are estimated using the full covariance matrix. The cell esds are taken into account individually in the estimation of esds in distances, angles and torsion angles; correlations between esds in cell parameters are only used when they are defined by crystal symmetry. An approximate (isotropic) treatment of cell esds is used for estimating esds involving l.s. planes.

Fractional atomic coordinates and isotropic or equivalent isotropic displacement parameters (Å²)

	x	*y*	*z*	U_{iso}*/U_{eq}
Ni1	0.500000	0.500000	0.500000	0.02724 (12)
Cl1	0.14959 (7)	−0.20644 (6)	0.64253 (6)	0.0683 (2)
N1	0.49579 (14)	0.68437 (13)	0.49747 (12)	0.0302 (4)
N2	0.14853 (18)	0.02547 (18)	0.65643 (15)	0.0489 (5)
O1	0.63069 (14)	0.50565 (11)	0.63625 (12)	0.0365 (3)
H11	0.6796 (16)	0.5604 (14)	0.6359 (19)	0.044*
H12	0.6766 (17)	0.4477 (13)	0.6434 (18)	0.044*
O2	0.35666 (14)	0.50182 (12)	0.60512 (12)	0.0381 (3)
H21	0.363 (2)	0.5067 (18)	0.6729 (8)	0.046*
H22	0.2918 (13)	0.4706 (19)	0.5828 (17)	0.046*
O3	0.21575 (15)	0.29848 (13)	0.36561 (13)	0.0513 (4)
O4	0.15477 (15)	0.36711 (14)	0.52437 (14)	0.0577 (5)
O5	0.77684 (18)	0.31004 (15)	0.67043 (15)	0.0578 (5)
H51	0.765 (2)	0.280 (2)	0.7309 (13)	0.069*
H52	0.8451 (14)	0.341 (2)	0.670 (2)	0.069*
O6	−0.02489 (19)	0.4641 (2)	0.64545 (15)	0.0691 (5)
H61	0.027 (2)	0.434 (2)	0.608 (2)	0.083*
H62	−0.063 (2)	0.511 (2)	0.604 (2)	0.083*
C1	0.5043 (2)	0.74728 (16)	0.40446 (16)	0.0366 (5)
H1	0.509493	0.706173	0.337893	0.044*
C2	0.5057 (2)	0.86964 (16)	0.40158 (16)	0.0368 (5)
H2	0.511821	0.909144	0.334314	0.044*
C3	0.49798 (17)	0.93401 (15)	0.49898 (15)	0.0280 (4)
C4	0.48697 (19)	0.86865 (16)	0.59518 (16)	0.0361 (5)
H4	0.480202	0.907506	0.662667	0.043*
C5	0.48605 (19)	0.74622 (15)	0.59102 (16)	0.0359 (5)
H5	0.478228	0.704445	0.656807	0.043*
C6	0.1538 (2)	0.1347 (2)	0.61298 (18)	0.0456 (5)
H6	0.147862	0.199385	0.660541	0.055*
C7	0.16748 (18)	0.15756 (17)	0.50216 (16)	0.0356 (5)
C8	0.1733 (2)	0.06049 (18)	0.43203 (17)	0.0414 (5)
H8	0.180909	0.072105	0.356359	0.050*
C9	0.1679 (2)	−0.05304 (19)	0.47386 (18)	0.0439 (5)
H9	0.172347	−0.119476	0.428227	0.053*
C10	0.1557 (2)	−0.06397 (19)	0.58621 (18)	0.0429 (5)
C11	0.17917 (18)	0.28366 (18)	0.46017 (19)	0.0419 (5)

Atomic displacement parameters (Å²)

	U^{11}	U^{22}	U^{33}	U^{12}	U^{13}	U^{23}
Ni1	0.0411 (2)	0.01267 (17)	0.02797 (19)	−0.00048 (13)	0.00315 (14)	0.00009 (12)
Cl1	0.0830 (5)	0.0554 (4)	0.0687 (4)	0.0079 (3)	0.0195 (4)	0.0253 (3)
N1	0.0420 (9)	0.0166 (7)	0.0319 (8)	0.0007 (6)	0.0030 (7)	−0.0009 (6)
N2	0.0538 (12)	0.0589 (12)	0.0347 (10)	−0.0021 (9)	0.0074 (9)	0.0018 (9)
O1	0.0476 (9)	0.0236 (7)	0.0370 (8)	−0.0015 (6)	−0.0024 (7)	0.0019 (6)
O2	0.0462 (9)	0.0351 (8)	0.0340 (7)	−0.0063 (6)	0.0083 (7)	−0.0039 (6)
O3	0.0695 (11)	0.0353 (8)	0.0500 (10)	−0.0096 (7)	0.0104 (8)	−0.0005 (7)
O4	0.0557 (10)	0.0410 (9)	0.0795 (12)	−0.0068 (7)	0.0228 (9)	−0.0210 (8)
O5	0.0731 (13)	0.0458 (10)	0.0537 (10)	0.0071 (8)	0.0020 (10)	0.0065 (8)
O6	0.0751 (14)	0.0873 (14)	0.0481 (10)	0.0270 (10)	0.0226 (10)	0.0193 (9)
C1	0.0597 (14)	0.0203 (9)	0.0305 (10)	−0.0001 (8)	0.0075 (10)	−0.0023 (8)
C2	0.0601 (14)	0.0186 (9)	0.0325 (11)	−0.0011 (8)	0.0082 (10)	0.0023 (8)
C3	0.0325 (10)	0.0169 (9)	0.0346 (10)	0.0011 (7)	0.0023 (8)	0.0008 (7)
C4	0.0578 (13)	0.0201 (9)	0.0308 (10)	0.0006 (8)	0.0061 (9)	−0.0036 (8)
C5	0.0570 (13)	0.0190 (9)	0.0321 (11)	−0.0002 (8)	0.0057 (9)	0.0042 (8)
C6	0.0457 (13)	0.0504 (14)	0.0410 (12)	−0.0061 (10)	0.0055 (10)	−0.0107 (10)
C7	0.0318 (11)	0.0374 (11)	0.0376 (11)	−0.0035 (8)	0.0039 (9)	−0.0055 (9)
C8	0.0526 (14)	0.0384 (12)	0.0340 (11)	−0.0028 (10)	0.0081 (10)	−0.0004 (9)
C9	0.0543 (14)	0.0353 (11)	0.0432 (13)	0.0000 (10)	0.0094 (11)	−0.0036 (10)
C10	0.0408 (13)	0.0447 (13)	0.0440 (13)	0.0027 (9)	0.0080 (10)	0.0089 (10)
C11	0.0326 (12)	0.0358 (11)	0.0570 (14)	−0.0041 (9)	0.0032 (10)	−0.0103 (10)

Geometric parameters (Å, º)

Ni1—O1^{i}	2.0643 (15)	O6—H61	0.818 (10)
Ni1—O1	2.0643 (15)	O6—H62	0.813 (10)
Ni1—N1^{i}	2.0715 (14)	C1—C2	1.375 (3)
Ni1—N1	2.0715 (14)	C1—H1	0.9300
Ni1—O2^{i}	2.0850 (13)	C2—C3	1.385 (2)
Ni1—O2	2.0850 (13)	C2—H2	0.9300
Cl1—C10	1.741 (2)	C3—C4	1.384 (2)
N1—C1	1.333 (2)	C3—C3^{ii}	1.483 (3)
N1—C5	1.334 (2)	C4—C5	1.376 (3)
N2—C10	1.319 (3)	C4—H4	0.9300
N2—C6	1.337 (3)	C5—H5	0.9300
O1—H11	0.811 (9)	C6—C7	1.378 (3)
O1—H12	0.818 (9)	C6—H6	0.9300
O2—H21	0.813 (9)	C7—C8	1.383 (3)
O2—H22	0.807 (10)	C7—C11	1.513 (3)
O3—C11	1.248 (2)	C8—C9	1.374 (3)
O4—C11	1.257 (2)	C8—H8	0.9300
O5—H51	0.822 (10)	C9—C10	1.375 (3)
O5—H52	0.815 (10)	C9—H9	0.9300
O1^{i}—Ni1—O1	180.0	C1—C2—C3	119.92 (17)

O1^{i}—Ni1—N1^{i}	89.62 (6)	C1—C2—H2	120.0
O1—Ni1—N1^{i}	90.37 (6)	C3—C2—H2	120.0
O1^{i}—Ni1—N1	90.38 (6)	C4—C3—C2	116.48 (16)
O1—Ni1—N1	89.62 (6)	C4—C3—C3^{ii}	121.39 (19)
N1^{i}—Ni1—N1	180.0	C2—C3—C3^{ii}	122.13 (19)
O1^{i}—Ni1—O2^{i}	90.61 (6)	C5—C4—C3	120.04 (17)
O1—Ni1—O2^{i}	89.39 (6)	C5—C4—H4	120.0
N1^{i}—Ni1—O2^{i}	89.00 (5)	C3—C4—H4	120.0
N1—Ni1—O2^{i}	91.00 (5)	N1—C5—C4	123.37 (17)
O1^{i}—Ni1—O2	89.39 (6)	N1—C5—H5	118.3
O1—Ni1—O2	90.61 (6)	C4—C5—H5	118.3
N1^{i}—Ni1—O2	91.00 (5)	N2—C6—C7	124.1 (2)
N1—Ni1—O2	89.00 (5)	N2—C6—H6	117.9
O2^{i}—Ni1—O2	180.0	C7—C6—H6	117.9
C1—N1—C5	116.61 (16)	C6—C7—C8	117.23 (19)
C1—N1—Ni1	122.63 (12)	C6—C7—C11	121.10 (18)
C5—N1—Ni1	120.76 (12)	C8—C7—C11	121.65 (18)
C10—N2—C6	116.23 (18)	C9—C8—C7	120.18 (19)
Ni1—O1—H11	114.7 (16)	C9—C8—H8	119.9
Ni1—O1—H12	115.0 (16)	C7—C8—H8	119.9
H11—O1—H12	102 (2)	C8—C9—C10	117.0 (2)
Ni1—O2—H21	127.6 (17)	C8—C9—H9	121.5
Ni1—O2—H22	117.6 (16)	C10—C9—H9	121.5
H21—O2—H22	111 (2)	N2—C10—C9	125.3 (2)
H51—O5—H52	113 (3)	N2—C10—Cl1	116.40 (16)
H61—O6—H62	105 (3)	C9—C10—Cl1	118.34 (17)
N1—C1—C2	123.56 (17)	O3—C11—O4	124.1 (2)
N1—C1—H1	118.2	O3—C11—C7	118.15 (17)
C2—C1—H1	118.2	O4—C11—C7	117.69 (19)

C5—N1—C1—C2	1.2 (3)	N2—C6—C7—C11	−176.9 (2)
Ni1—N1—C1—C2	−177.83 (16)	C6—C7—C8—C9	−1.2 (3)
N1—C1—C2—C3	0.0 (3)	C11—C7—C8—C9	177.10 (19)
C1—C2—C3—C4	−1.1 (3)	C7—C8—C9—C10	0.5 (3)
C1—C2—C3—C3^{ii}	178.6 (2)	C6—N2—C10—C9	0.0 (3)
C2—C3—C4—C5	1.0 (3)	C6—N2—C10—Cl1	179.70 (16)
C3^{ii}—C3—C4—C5	−178.7 (2)	C8—C9—C10—N2	0.1 (3)
C1—N1—C5—C4	−1.3 (3)	C8—C9—C10—Cl1	−179.55 (16)
Ni1—N1—C5—C4	177.75 (16)	C6—C7—C11—O3	166.0 (2)
C3—C4—C5—N1	0.2 (3)	C8—C7—C11—O3	−12.3 (3)
C10—N2—C6—C7	−0.8 (3)	C6—C7—C11—O4	−12.0 (3)
N2—C6—C7—C8	1.4 (3)	C8—C7—C11—O4	169.7 (2)

Symmetry codes: (i) −*x*+1, −*y*+1, −*z*+1; (ii) −*x*+1, −*y*+2, −*z*+1.

Hydrogen-bond geometry (Å, º)

D—H···*A*	*D*—H	H···*A*	*D*···*A*	*D*—H···*A*
O1—H11···O3^{i}	0.81 (1)	1.95 (1)	2.756 (2)	175 (2)

O1—H12···O5	0.82 (1)	1.90 (1)	2.715 (2)	175 (2)
O2—H21···N2^{iii}	0.81 (1)	2.08 (1)	2.885 (2)	172 (2)
O2—H22···O4	0.81 (1)	1.96 (1)	2.757 (2)	169 (2)
O5—H51···O3^{iv}	0.82 (1)	1.96 (1)	2.776 (2)	172 (3)
O5—H52···O6^{v}	0.82 (1)	2.01 (1)	2.790 (3)	160 (3)
O6—H61···O4	0.82 (1)	1.94 (1)	2.753 (2)	177 (3)
O6—H62···O4^{vi}	0.81 (1)	2.23 (1)	3.035 (3)	174 (3)
C4—H4···O6^{iii}	0.93	2.40	3.288 (3)	160
C9—H9···O5^{vii}	0.93	2.53	3.447 (3)	169

Symmetry codes: (i) −*x*+1, −*y*+1, −*z*+1; (iii) −*x*+1/2, *y*+1/2, −*z*+3/2; (iv) *x*+1/2, −*y*+1/2, *z*+1/2; (v) *x*+1, *y*, *z*; (vi) −*x*, −*y*+1, −*z*+1; (vii) −*x*+1, −*y*, −*z*+1.